Non-Landau critical behavior of heat capacity at the smectic-A–smectic-C_α^* transition of the antiferroelectric liquid crystal methylheptyloxycarbonylphenyl octyloxycarbonylbiphenyl carboxylate

Kenji Ema and Haruhiko Yao
Department of Physics, Faculty of Science, Tokyo Institute of Technology, 2-12-1 Oh-okayama, Meguro, Tokyo, 152 Japan

Atsuo Fukuda, Yoichi Takanishi, and Hideo Takezoe
Department of Organic and Polymeric Materials, Faculty of Engineering, Tokyo Institute of Technology, 2-12-1 Oh-okayama, Meguro, Tokyo, 152 Japan

(Received 14 May 1996)

High resolution ac calorimetric measurements have been carried out near the smectic-A–smectic-C_α^* phase transition in an antiferroelectric liquid crystal 4-(1-methylheptyloxycarbonyl)phenyl 4′-octyloxycarbonylbiphenyl-4-carboxylate. A clear deviation from the extended mean-field Landau behavior was seen. The data have been analyzed using a renormalization-group expression including the correction-to-scaling terms. It was found that the heat-capacity anomaly can be described with the three-dimensional XY model, in agreement with the theoretical prediction. [S1063-651X(96)04010-X]

PACS number(s): 61.30.−v, 64.70.Md, 64.60.Fr, 65.20.+w

I. INTRODUCTION

Theoretically, the smectic-A (Sm-A)–smectic-C (Sm-C) transition and the smectic-A–chiral-smectic-C (Sm-C*) transition belong to the three-dimensional (3D) XY universality class [1]. On the other hand, experimentally observed data on the heat capacity, the tilt order parameter, the susceptibility, etc. at the Sm-A–Sm-C (or C*) transitions are classified into two types. Almost all data belong to the first type, which are well described by the extended Landau theory which includes up to sixth-order terms of the tilt order parameter (see Refs. [2–5], and also references therein). Conversely, only a few cases belong to the second type, which show a clear deviation from the Landau behavior [6–9].

An interesting contrast has been found in two antiferroelectric liquid crystals recently studied by the present authors. They are 4-(1-methylheptyloxycarbonyl)phenyl 4′-octyloxybiphenyl-4-carboxylate (MHPOBC), and its octyloxycarbonylbiphenyl analog (MHPOCBC). The sequences of phase transitions for these compounds are

$$\text{Sm-}C_A^* \overset{391.6.\ \text{K}}{\longleftrightarrow} \text{Sm-}C_\gamma^* \overset{392.4\ \text{K}}{\longleftrightarrow} \text{Sm-}C^* \overset{394.1\ \text{K}}{\longleftrightarrow} \text{Sm-}C_\alpha^* \overset{395.2\ \text{K}}{\longleftrightarrow} \text{Sm-}A \overset{421\ \text{K}}{\longleftrightarrow} I$$

for MHPOBC [10–12], and

$$\text{Sm-}C_A^* \overset{372.7\ \text{K}}{\longleftrightarrow} \text{Sm-}C_\alpha^* \overset{378.7\ \text{K}}{\longleftrightarrow} \text{Sm-}A \overset{420\ \text{K}}{\longleftrightarrow} I$$

for MHPOCBC [13]. Here Sm-A is a paraelectric phase, Sm-C* is a ferroelectric phase, Sm-C_α^* and Sm-C_A^* are antiferroelectric phases, and Sm-C_γ^* is a ferrielectric phase, and I stands for the isotropic phase. While the heat-capacity anomaly accompanying the Sm-A–Sm-C_α^* transition in MHPOBC shows a clear deviation from mean-field Landau behavior [14], no noticable deviation from the Landau behavior was observed in the case of MHPOCBC [15]. This contrast is remarkable, since the two compounds have almost the same molecular structure, with only one extra carbonyl group in MHPOCBC. However, because the overall magnitude of the heat anomaly is quite small in MHPOCBC, being about one fifth of that in MHPOBC, care should be taken to exclude the existence of any deviation from the Landau behavior which might be very small. In this paper we report the results of our most recent ac calorimetric measurement on MHPOCBC with improved precision. The results described below reveal that the anomaly is not explained by the extended Landau theory.

II. METHOD AND RESULTS

The ac calorimeter used is described elsewhere [16,17]. The present setup of the calorimeter enables us to obtain heat-capacity data with a precision of about ±0.010% (this value quotes the standard deviation in the total heat capacity, including that of the empty cell). The scan rate of the sample temperature is about 45 mK/h near the transition temperature. Measurements were made on two sample cells, including several heating and cooling runs for each of them, which gave an excellent reproducibility.

Figure 1 shows the temperature dependence of the heat capacity C_p obtained on cooling. The dashed line shows the

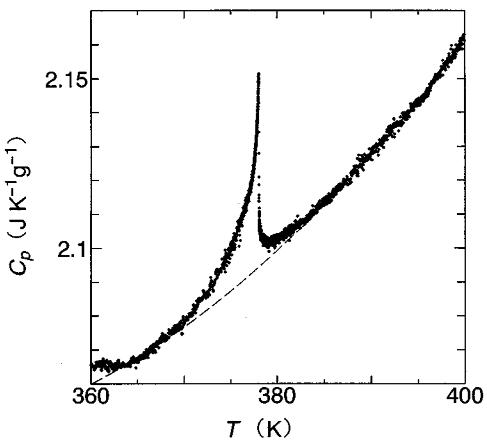

FIG. 1. Overall temperature dependence of the heat capacity C_p of MHPOCBC. The dashed line shows the background heat capacity (see text).

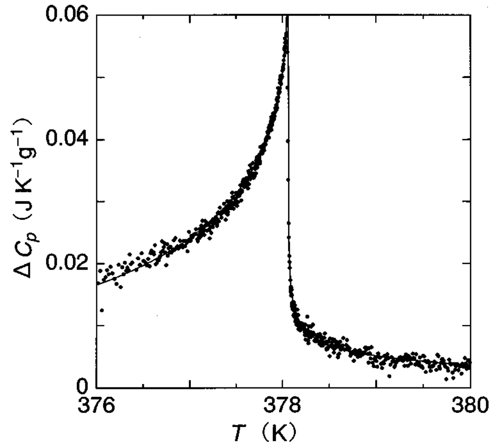

FIG. 2. Detailed view of the excess heat capacity ΔC_p near the Sm-A–Sm-C_α^* phase transition of MHPOCBC. Solid line shows the theoretical 3D XY fit with Eq. (1) (see text).

normal part of the heat capacity determined as a quadratic function of the temperature, so that the excess part goes smoothly to zero at temperatures far away from the transition on the both sides. The results were identical in other runs irrespective of heating or cooling, except for a very small shift in the temperature scales due to the drift in transition temperatures with a rate of about -2.4 mK/day. Because the overall magnitude of the heat anomaly is quite small, it is not certain in Fig. 1 whether any excess heat capacity exists in the Sm-A phase. After subtracting the normal part, the anomalous heat capacity ΔC_p is plotted on enlarged scales in Fig. 2. The existence of excess heat capacity in the Sm-A phase is now clear. Thus we see MHPOCBC also shows a non-Landau critical behavior. From Fig. 2 of the present data and Fig. 1 of Ref. [15], it is seen that the relative magnitude of the anomaly above T_c and the peak at T_c are similar to each other for MHPOCBC and MHPOBC. However, the C_p peak height in MHPOCBC is about one fifth of that in MHPOBC. As a result, while the excess heat capacity at T_c+ 1 K is about 1 % of the total heat capacity in MHPOBC, it is only about 0.2% of C_p in MHPOCBC, and falls within the experimental uncertainty in our former result.

III. DATA ANALYSIS

The ΔC_p data have been analyzed with the following renormalization-group expression, including the corrections-to-scaling terms [18]:

$$\Delta C_p = A^{\pm}|t|^{-\alpha}(1+D_1^{\pm}|t|^{\Delta_1}+D_2^{\pm}|t|)+B_c, \qquad (1)$$

where $t\equiv(T-T_c)/T_c$ is the reduced temperature, and the superscripts $\pm$ denote above and below T_c. The second-order correction term $D_2^{\pm}|t|$ is actually a combination of several higher-order terms that have almost the same t dependence [19,20]. There is usually a narrow region very close to T_c where data are artificially rounded due to impurities or instrumental effects. The extent of this region was carefully determined in a way described elsewhere [21], and the data inside this region were excluded in the fitting. The rounding region thus determined is typically $-7\times10^{-5}<t<+1\times10^{-5}$.

At first, the exponent α was adjusted freely in the least-squares calculation. The correction-to-scaling exponent Δ_1 is actually system dependent, but has a value quite close to 0.5 as far as theoretically known (0.524 for the 3D XY model, and 0.496 for the 3D Ising model [18]). Therefore, we fixed its value to 0.5 in this stage of fitting. The coefficients $D_2^{\pm}$ were held fixed at zero. Fits were made for the data over three ranges, $|t|_{\max}$ = 0.001, 0.003, and 0.01, where $|t|_{\max}$ is the maximum value of $|t|$ used in the fit. In Table I, the first three lines show the values of the critical exponent α, the critical amplitude ratio A^-/A^+, and other adjustable parameters thus obtained. It is seen that the fits yield an α close to the 3D XY value of -0.0066 [18] for $|t|_{\max}$ = 0.001, while larger values are obtained for larger $|t|_{\max}$.

TABLE I. Least-squares values of the adjustable parameters for fitting ΔC_p with Eq. (1). Quantities in brackets were held fixed at the given values. In the 3D XY fits, the exponent Δ_1 has been held fixed to the theoretical value. The units for A^+ and B_c are J K^{-1} g^{-1}.

$\lvert t\rvert_{\max}$	T_c (K)	α	A^+	A^-/A^+	D_1^+	D_1^-	B_c	ν	χ_ν^2
0.001	378.072	0.004	0.8807	1.053	0.131	-0.568	-0.9014	226	1.00
0.003	378.074	0.084	0.01260	2.736	-2.52	-6.54	-0.0134	460	1.30
0.010	378.073	0.120	0.00742	3.121	-1.804	-5.47	-0.0088	800	2.07
0.001	378.070	[-0.0066]	-0.6564	0.922	-0.301	1.059	0.6298	227	1.00
0.003	378.058	[-0.0066]	-0.7566	0.941	-0.208	0.580	0.7260	461	1.63
0.010	378.049	[-0.0066]	-0.8555	0.954	-0.164	0.293	0.8208	801	3.56

TABLE II. Least-squares values of the adjustable parameters for fitting ΔC_p with Eq. (1). Quantities in brackets were held fixed at the given values. The exponent Δ_1 has been held fixed to the theoretical value for the 3D XY model. The units for A^+ and B_c are J K^{-1} g^{-1}.

$\|t\|_{max}$	T_c (K)	α	A^+	A^-/A^+	D_1^+	D_1^-	D_2^+	D_2^-	B_c	ν	χ_ν^2
0.003	378.072	[−0.0066]	−0.5993	0.909	−0.439	1.821	3.92	−11.3	0.5755	459	1.18
0.010	378.061	[−0.0066]	−0.7808	0.939	−0.322	0.760	1.39	−3.16	0.7479	799	2.08

We next fitted the data fixing the exponents α and Δ_1 to theoretically expected values for 3D XY models. The fourth through sixth lines in Table I show the results of such fits. Values of the universal amplitude ratio A^-/A^+ are stable against the data range shrinking, and agree well with the theoretical value ($A^-/A^+ = 0.971$ [22]).

Table II shows the results of the fitting when the second-order correction terms are included. Since higher-order correction terms have significant influence away from T_c, only the results for larger $|t|_{max}$ are shown. In Fig. 2, solid line shows the theoretical fit with 3D XY exponents to the data with $|t|_{max}=0.01$. It is seen that the agreement between observed and theoretically calculated values is fairly good. After all, the observed C_p anomaly is described adequately with the 3D XY model, in agreement with the theoretical expectation.

IV. DISCUSSION

The fitting results given in Tables I and II suggest that second-order correction plays an important role especially over a range as wide as $|t|_{max} = 0.01$. The values of $D_2^\pm$ are not so stable against the range that is shrinking, but it is expected that those for the wider range, $|t|_{max} = 0.01$, are more reliable. On the other hand, the D_1 values in Table I are slightly unstable, but in this case those with smaller $|t|_{max}$ are reliable since the effect from the second-order corrections has been renormalized into D_1 values for wider-range fits. Indeed, the $D_1^\pm$ in Table I for $|t|_{max} = 0.001$ agree well with those in Table II for $|t|_{max}=0.01$. Thus as the best estimates we obtain $D_1^+ \cong -0.3$ and $D_1^- \cong 0.8$–1.0. These values seem reasonable in the sense that they are of the order of unity, although the theoretical prediction that $D_1^+ = D_1^-$ [23] is not fulfilled. A similar tendency was seen in the case of MHPOBC [14]. It is likely that this is related to the existence of the crossover from 3D XY to tricritical behavior.

So far we have seen that MHPOBC and MHPOCBC both exhibit non-Landau critical heat anomaly. Also, in MHPBC, the octylbiphenyl analog of MHPOBC [24], a similar critical anomaly seems to exist (see Fig. 4 of Ref. [25]). Quite recently, the present authors found that a racemic mixture of MHPOBC shows a non-Landau tricritical behavior [26]. Thus a question arises why non-Landau critical behavior is seen in MHPOCBC and its related liquid crystals having antiferroelectric phases, in contrast to almost all other liquid crystals, which also undergo the Sm-A–Sm-C (or Sm-C*) phase transition. Since the racemic mixture of MHPOBC undergoes a Sm-A–Sm-C phase transition and still shows non-Landau behavior, the criticality is not specific to the antiferroelectricity or more particularly the antiferroelectric Sm-C_α^* phase. In Ref. [26], the present authors proposed two scenarios for explaining the criticality in MHPOBC-group antiferroelectric liquid crystals. (a) The coexistence of antiferroelectric- and ferroelectric interactions is the main cause of the non-Landau critical behavior in these materials. (b) The Landau behavior reported previously for MHPOCBC (which appeared to describe the data in Ref. [15]) can be understood by the wide temperature range of the Sm-A phase in this compound. The present result has shown that (b) is not the case. This adjustment, however, simplifies the overall situation because now we see that all three liquid crystals MHPOBC, MHPOCBC, and MHPBC, composed of quite similar molecules, exhibit equally non-Landau critical behaviors. Therefore the origin of critical behavior can be sought as a common feature for these compounds. Further experimental studies, including high-resolution x-ray measurements, are needed to be made on these systems.

ACKNOWLEDGMENTS

This work was partly supported by a Grant-in-Aid for Scientific Research (Specially Promoted Research No. 06102005) from the Ministry of Education, Science and Culture.

[1] P. G. de Gennes, Mol. Cryst. Liq. Cryst. **21**, 49 (1973).
[2] C. C. Huang and J. M. Viner, Phys. Rev. A **25**, 3385 (1982).
[3] C. C. Huang and S. Dumrongrattana, Phys. Rev. A **34**, 5020 (1986).
[4] T. Chan, Ch. Bahr, G. Heppke, and C. W. Garland, Liq. Cryst. **13**, 667 (1993).
[5] F. Yang, G. W. Bradberry, and J. R. Sambles, Phys. Rev. E **50**, 2834 (1994).
[6] M. Delaye, J. Phys. (Paris) Colloq. **40**, C3-350 (1979).
[7] L. Benguigui and P. Martinoty, Phys. Rev. Lett. **63**, 774 (1989).
[8] D. Collin, S. Moyses, M. E. Neubert, and P. Martinoty, Phys. Rev. Lett. **73**, 983 (1994).
[9] L. Reed, T. Stoebe, and C. C. Huang, Phys. Rev. E **52**, R2157 (1995).
[10] A. D. L. Chandani, Y. Ouchi, H. Takezoe, A. Fukuda, K. Terashima, K. Furukawa, and A. Kishi, Jpn. J. Appl. Phys. **28**, L1261 (1989).

[11] Y. Takanishi, K. Hiraoka, V. K. Agrawal, H. Takezoe, A. Fukuda, and M. Matsushita, Jpn. J. Appl. Phys. **30**, 2023 (1991).
[12] K. Hiraoka, Y. Takanishi, K. Skarp, H. Takezoe, and A. Fukuda, Jpn. J. Appl. Phys. **30**, L1819 (1991).
[13] T. Isozaki, Y. Suzuki, I. Kawamura, K. Mori, N. Yamamoto, Y. Yamada, H. Orihara, and Y. Ishibashi, Jpn. J. Appl. Phys. **30**, L1573 (1991); T. Isozaki, K. Hiraoka, Y. Takanishi, H. Takezoe, A. Fukuda, Y. Suzuki, and I. Kawamura, Liq. Cryst. **12**, 59 (1992).
[14] K. Ema, J. Watanabe, A. Takagi, and H. Yao, Phys. Rev. E **52**, 1216 (1995).
[15] K. Ema, H. Yao, I. Kawamura, T. Chan, and C. W. Garland, Phys. Rev. E **47**, 1203 (1993).
[16] K. Ema, T. Uematsu, A. Sugata, and H. Yao, Jpn. J. Appl. Phys. **32**, 1846 (1993).
[17] The details of the calorimeter are planned to be described in a review article in the near future.
[18] C. Bagnuls and C. Bervillier, Phys. Rev. B **32**, 7209 (1985); C. Bagnuls, C. Bervillier, D. I. Meiron, and B. G. Nickel, *ibid.* **35**, 3585 (1987).
[19] C. Bagnuls and C. Bervillier, Phys. Lett. **112A**, 9 (1985).
[20] C. W. Garland, G. Nounesis, M. J. Young, and R. J. Birgeneau, Phys. Rev. E **47**, 1918 (1993).
[21] H. Haga, A. Onodera, Y. Shiozaki, K. Ema, and H. Sakata, J. Phys. Soc. Jpn. **64**, 822 (1995).
[22] C. Bervillier, Phys. Rev. B **34**, 8141 (1986).
[23] A. Aharony and G. Ahlers, Phys. Rev. Lett. **44**, 782 (1980).
[24] N. Okabe, Y. Suzuki, I. Kawamura, T. Isozaki, H. Takezoe, and A. Fukuda, Jpn. J. Appl. Phys. **31**, L793 (1992).
[25] K. Ema, J. Watanabe, and H. Yao, Ferroelectrics **156**, 173 (1994).
[26] K. Ema, A. Takagi, and H. Yao, Phys. Rev. E **53**, R3036 (1996).